DFT Reinvestigation of DNA Strand Breaks Induced by Electron Attachment

ARTICLE *in* THE JOURNAL OF PHYSICAL CHEMISTRY B · SEPTEMBER 2014

Impact Factor: 3.3 · DOI: 10.1021/jp506679b · Source: PubMed

5 AUTHORS, INCLUDING:

Hsing-Yin Chen
Kaohsiung Medical University
43 PUBLICATIONS **835** CITATIONS

SEE PROFILE

THE JOURNAL OF PHYSICAL CHEMISTRY B

Article

pubs.acs.org/JPCB

DFT Reinvestigation of DNA Strand Breaks Induced by Electron Attachment

Hsing-Yin Chen,* Po-Yu Yang, Hui-Fen Chen, Chai-Lin Kao, and Li-Wenm Liao

Department of Medicinal and Applied Chemistry, Kaohsiung Medical University, Kaohsiung 807, Taiwan

Supporting Information

ABSTRACT: The benchmark study of DFT methods on the activation energies of phosphodiester C3′−O and C5′−O bond ruptures and glycosidic C1′−N bond ruptures induced by electron attachment was performed. While conventional pure and hybrid functionals provide a relatively reasonable description for the C1′−N bond rupture, they significantly underestimate the energy barriers of the C−O bond ruptures. This is because the transition states of the later reactions, which are characterized by an electron distribution delocalized from the nucleobase to sugar−phosphate backbone, suffer from a severe self-interaction error in common DFT methods. CAM-B3LYP, M06-2X, and ωB97XD are the top three methods that emerged from the benchmark study; the mean absolute errors relative to the CCSD(T) values are 1.7, 1.9, and 2.2 kcal/mol, respectively. The C−O bond cleavages of 3′- and 5′-dXMP$^{\bullet-}$, where X represents four nucleobases, were then recalculated at the M06-2X/6-31++G**//M06-2X/6-31+G* level, and it turned out that the C−O bond cleavages do not proceed as easily as previously predicted by the B3LYP calculations. Our calculations revealed that the C−O bonds of purine nucleotides are more susceptible than pyrimidine nucleotides to the electron attachment. The energies of electron attachment to nucleotides were calculated and discussed as well.

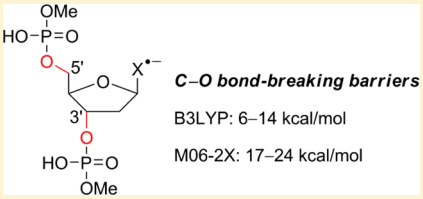

INTRODUCTION

Radiation damage to DNA can occur either by a direct route or indirect route. In the direct route, radiation directly interacts with DNA and deposits energy on it. However, ∼80% of the composition of a cell is water; as a consequence, when a cell is subjected to irradiation, most of the radiation energy is absorbed by water rather than by DNA. The radiolysis of water produces reactive free radicals including hydroxyl radicals, hydrogen radicals, and peroxyl radicals. The DNA damage caused by the chemical species generated during the radiolysis of water belongs to the indirect route.[1] The effects of these radicals on DNA damage have been extensively investigated and reasonably well understood.[2−5]

Besides the above-mentioned radicals, a large number of free electrons are also created by the radiolysis of water.[2] Yet, the role of free electrons in DNA damage has long been disregarded. Until 2000, a seminal work conducted by Boudaïffa et al. clearly demonstrated that low-energy electrons (LEEs) of 3−20 eV are able to trigger single- and double-strand breaks (SSBs and DSBs) of dry DNA thin film in vacuum.[6] A later study further showed that even 0−4 eV electrons can induce SSBs, with the maximum yield at ∼1 eV; however, DSBs were not observed within this energy range.[7] Simulations of the profile of SSBs based on the resonance energies of nucleobases support that DNA strand breaks induced by 0−4 eV electrons are initiated by electron attachment to nucleobase moieties.[7] These pioneering works kindled a great interest in the area of LEE-induced DNA damage. Over the past decade, myriads of gas-phase and solid-phase experiments and theoretical studies regarding the interactions of electrons with various DNA subunits or with DNA have been reported. These studies have shown that LEEs can trigger a variety of chemical reactions detrimental to DNA, such as sugar−phosphate bond cleavage,[8−13] glycosidic bond cleavage,[8−16] decomposition of nucleobases,[17−23] tautomerization of nucleobases,[24−31] and decomposition of ribose.[12,32−34]

While the aforementioned gas-phase and solid-phase experiments are instructive and stimulate the development of the research field of LEE damage to DNA, these experimental results are less relevant to biology due to the absence of an aqueous environment. Earlier work showed that the aqueous electron has only a small effect on DNA damage, in particular, in vivo conditions where competing reactions of electrons with other species dissolved in water can take place.[2,35] Recently, by using femtosecond time-resolved laser spectroscopy, Lu and co-workers have successfully created excess electrons via two-photon photolysis of water and investigated the subsequent reactions of excess electrons with nucleotides[36] and DNA[37] in aqueous solutions. They found that adenine and cytosine nucleotides can capture aqueous electrons to form stable anions, whereas electron attachment to guanine and thymine nucleotides results in rapid bond dissociations. Although it is not clear which bonds are broken, the experimental data led the authors to exclude the possibility of sugar−phosphate bond cleavage and support direction dissociation on nucleobase moieties.[36] They further demonstrated that electrons can cause SSBs and DSBs of DNA in aqueous environment. Surprisingly, they inferred that, from the measurements of DNA strand

Received: July 4, 2014
Revised: September 2, 2014
Published: September 3, 2014

   dx.doi.org/10.1021/jp506679b | J. Phys. Chem. B 2014, 118, 11137−11144

breaks with various scavengers, reductive damage induced by electrons is more effective than oxidative damage induced by $OH^{\bullet}$ radicals.[37] This brand new and far-reaching finding challenges the conventional wisdom that radiation damage to DNA mainly comes from the oxidation by $OH^{\bullet}$ radicals.[38]

The mechanisms of DNA strand breaks caused by LEEs have been intensively studied by using ab initio Hartree−Fock[39−44] and density functional theory (DFT) calculations.[44−54] These calculations reveal that 0−2 eV electrons initially attach to the π^* orbital of base moieties. During the stretching of the sugar−phosphate C−O bond, the excess electron transfers from the π^* of base to the σ^* of a distant C−O bond, which in turn promotes the DNA strand break. The excess electron on nucleobases can also delocalize to the σ^* of neighboring C1′−N bonds that connect base and sugar moieties, resulting in glycosidic bond cleavages and base releases.[52,55] In Table 1, we summarize the previous DFT results for the activation energies of C−O bond and C1′−N bond ruptures induced by electron attachment to 2′-deoxyribonucleoside 3′- or 5′-monophosphate (3′- or 5′-dXMP) and 2′-deoxyribonucleoside 3′,5′-diphosphate (3′,5′-dXDP). These data indicate that the sugar−phosphate C−O bonds are extremely vulnerable to electron attachment; for example, the C3′−O bond cleavages for cytosine and thymine nucleotide radical anions only need to surmount an energy barrier of 6−7 kcal/mol in the gas phase,[44,45] and the C−O bond cleavages for 3′,5′-$dGDP^{\bullet-}$ only need to surmount an energy barrier of 1−4 kcal/mol in the aqueous solution.[47] In contrast, the activation energies of glycosidic C1′−N bond cleavages were found to be much higher than those of C−O bond cleavages. The strand breaks induced by direct electron attachment on the DNA backbone have also been theoretically studied using a sugar−phosphate−sugar model; the barrier height of this process was found to be ∼10 kcal/mol.[56]

Table 1. Previous B3LYP Activation Energies (kcal/mol) for Phosphodiester and Glycosidic Bond Cleavages Induced by Electron Attachment[a]

model	C3′−O	C5′−O	C1′−N
3′- or 5′-dCMP	6.17 (12.82)[b]	14.27 (17.97)[f]	21.6[h]
		8.7 (6.6)[i]	25.3 (12.1)[i]
3′,5′-dCDP	6.03 (13.36)[j]	14.17 (18.73)[j]	26.21 (26.34)[j]
3′- or 5′- dTMP	7.06 (13.73)[b]	13.84 (17.86)[f]	18.9[h]
		13.5 (28.9)[g]	22.8 (17.5)[i]
		9.8 (14.1)[i]	
3′,5′-dTDP	6.04 (14.18)[j]	13.39 (18.76)[j]	19.19 (28.77)[j]
3′-dGMP	10.28 (5.25, 6.54)[c]		
3′,5′-dGDP	11.23 (3.56)[d]	12.97 (1.06)[d]	24.08 (9.99)[d]
3′,5′-dADP	8.94 (13.22)[e]	9.99 (22.54)[e]	21.29 (20.91)[e]

[a]Results without zero-point energy corrections, and the values in parentheses are aqueous-phase results. [b]Reference 45. [c]Reference 51. [d]Reference 47. [e]Reference 48. [f]Reference 44. [g]Reference 49. [h]Reference 52. [i]Reference 50. [j]Reference 46.

We noticed that all of the previous DFT studies exclusively adopted the B3LYP hybrid functional method, and we suspected that these B3LYP results might be problematic based on the following considerations. According to the previous B3LYP calculations, the C1′−N bond cleavages should be suppressed by the C−O bond cleavages; nevertheless, both bond-breaking reactions were detected in the thin-film and gas-phase experiments.[8−12] In addition, the transition states of the C−O bond-breaking reactions involve an excess electron distribution delocalized from the nucleobase to sugar−phosphate backbone (see molecular orbital plots in refs 43−53 and Figures S1 and S2 in the Supporting Information). It is well-established that conventional exchange−correlation (XC) functionals, like B3LYP, suffer from one-electron self-interaction error (also called delocalization error) and tend to overstabilize charge delocalized states.[57,58] Thus, it seems likely that the barrier heights of the C−O bond cleavages would be underestimated by the B3LYP method. In fact, this deficiency of the B3LYP method has already been noticed by Sevilla and co-workers.[59] They employed the BH&HLYP functional to compute the strand breaks in 5′-$dTMP^{\bullet-}$ and found that the vertical and adiabatic C−O bond-breaking barriers are 18.7 and 23.3 kcal/mol, respectively,[59] considerably higher than the B3LYP-computed values of 9 and 14.8 kcal/mol.[49]

Accordingly, we thought a DFT reinvestigation of excess-electron-induced DNA strand breaks is necessary. In this work, we present the first benchmark study of DFT functionals for the activation energies of C3′−O and C5′−O bond cleavages in 3′-$dTMP^{\bullet-}$ and 5′-$dTMP^{\bullet-}$ and C1′−N bond cleavage in the radical anion of thymine nucleoside $dT^{\bullet-}$. The results of the benchmark study validate our inference that conventional XC functionals are inadequate to describe the C−O bond-breaking reactions triggered by electron transfer. We then selected the M06-2X functional from the benchmark study to recalculate the C−O bond-breaking reactions in 3′- and 5′-$dXMP^{\bullet-}$ (X = A, G, T, C). It turned out that the C−O bond cleavages are not as easy as previously predicted by the B3LYP method.

COMUPATIONAL METHODS

The phosphate group of nucleotides was terminated by the methyl group, and the negative charge on it was neutralized by a proton. For the benchmark study, the performance of different types of DFT functionals, including pure functionals (BLYP,[60,61] PBE,[62,63] M06-L[64]), hybrid functionals (B3LYP,[61,65] PBE0,[66] B98[67]), hybrid meta functionals (M06,[68] M06-2X,[64] M06-HF[69]), and long-range corrected[70] functionals (LC-BLYP, LC-PBE, LC-M06-L, CAM-B3LYP,[71] ωB97XD[72]), on the activation energies of phosphodiester bond cleavage and glycosidic bond cleavage was assessed. The activation energies were evaluated by single-point energy calculations using the aforementioned functionals in combination with the 6-31+G* basis set on the B3LYP/6-31+G*-optimized geometries. High-level ab initio CCSD(T) results were taken as the reference values.

For the following study of electron attachment to nucleotides and the subsequent phosphodiester bond cleavages, the geometry optimizations and vibrational frequency calculations were performed at M06-2X/6-31+G* level. Single-point energy calculations with a larger basis set 6-31++G** were used to obtain more accurate energies. Our preliminary test showed that the M06-2X/6-31++G**//M06-2X/6-31+G* calculations give almost the same results as the M06-2X/6-31++G** calculations for the activation energies of C−O bond cleavages in nucleotide radical anions. We did not thoroughly employ the M06-2X/6-31++G** method in the present study because the optimized structures at this level for some systems display imaginary low-frequency vibrations that cannot be eliminated with efforts (see Table S1 in the Supporting Information).

To locate the transition states of the bond-breaking reactions, relaxed potential energy surface scans with increasing associated bond lengths were first carried out, and the geometries of the

dx.doi.org/10.1021/jp506679b | J. Phys. Chem. B 2014, 118, 11137−11144

maxima along the potential energy curves were then used as the initial guesses for the following transition-state geometry optimizations. The adequacy of the obtained transition states can be easily justified by the animation of imaginary vibration modes, which clearly displays a stretching motion along the bond-breaking coordinate.

The SMD continuum solvation model[73] was adopted to simulate the aqueous environment. The hydration effect was taken into account in two ways; one is using aqueous-phase single-point energy calculations on the gas-phase geometries, and the other is performing geometry optimizations directly in the aqueous environment. Free-energy corrections were made at standard conditions of 1 atm and 298.15 K. All calculations were accomplished by the Gaussian 09 package.[74]

RESULTS AND DISCUSSION

Benchmark Study. The radical anions of thymine nucleotides (3′-dTMP$^{\bullet-}$ and 5′-dTMP$^{\bullet-}$) and thymine nucleoside (dT$^{\bullet-}$) were used as models in the benchmark study for the activation energies of C3′−O, C5′−O, and C1′−N bond cleavages. The calculated activation energies are summarized in Table 2. The error for each bond-breaking reaction and the average unsigned error for the three reactions are illustrated in Figures 1 and 2, respectively.

Table 2. Activation Energies (kcal/mol) of Phosphodiester Bond Cleavages in 3′- and 5′-dTMP$^{\bullet-}$ and Glycosidic Bond Cleavages in dT$^{\bullet-}$ and Mean Absolute Errors Relative to CCSD(T) Values

	C3′−O	C5′−O	C1′−N	MAE
BLYP	3.7	5.9	17.2	10.9
PBE	5.3	7.5	20.3	8.8
M06-L	4.6	10.1	21.6	7.7
LC-BLYP	19.4	24.9	33.3	6.0
LC-PBE	21.3	26.7	35.8	8.1
LC-M06-L	19.7	23.2	34.1	5.8
B3LYP	8.6	13.7	21.9	5.1
PBE0	11.8	17.4	25.4	2.9
B98	9.6	15.1	22.8	4.0
CAM-B3LYP	15.6	22.3	26.7	1.7
M06	11.7	17.3	23.8	2.4
M06-2X	16.3	22.4	26.6	1.9
M06-HF	17.8	22.1	29.7	3.4
ωB97XD	15.9	22.2	27.9	2.2
CCSD(T)	15.1	20.9	23.5	

We tested the performance of pure XC functionals BLYP, PBE, and M06-L because pure functionals have much lower computational costs and, hence, are applicable to large molecular systems and molecular dynamics simulations. In fact, DFT-based molecular dynamics simulations using BLYP and PBE functionals have been carried out to study DNA strand breaks induced by electron attachment in aqueous environment.[75,76] However, our benchmark study revealed that pure XC functionals are catastrophic in predicting the barrier heights of C3′−O and C5′−O bond ruptures; these pure functionals significantly underestimate the barrier heights of C3′−O bond rupture by ∼10 kcal/mol and C5′−O bond rupture by 11−15 kcal/mol. Adding the long-range correction[70] to the pure functionals (LC-BLYP, LC-PBE, LC-M06-L), although leading to overcorrection, reduces the error to 4−6 kcal/mol for C3′−O bond rupture and to 2−6 kcal/mol for C5′−O bond rupture.

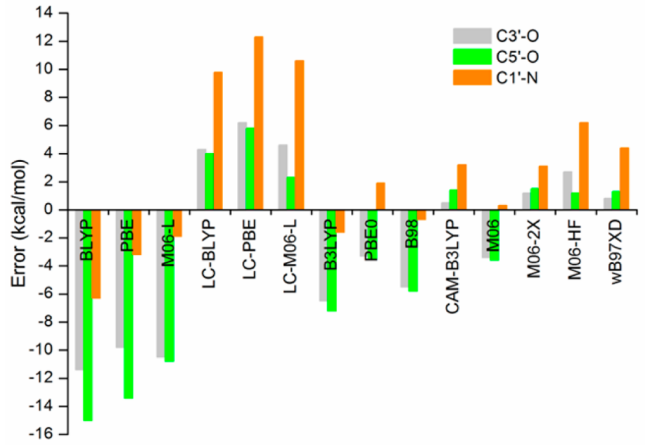

Figure 1. Errors relative to CCSD(T) results.

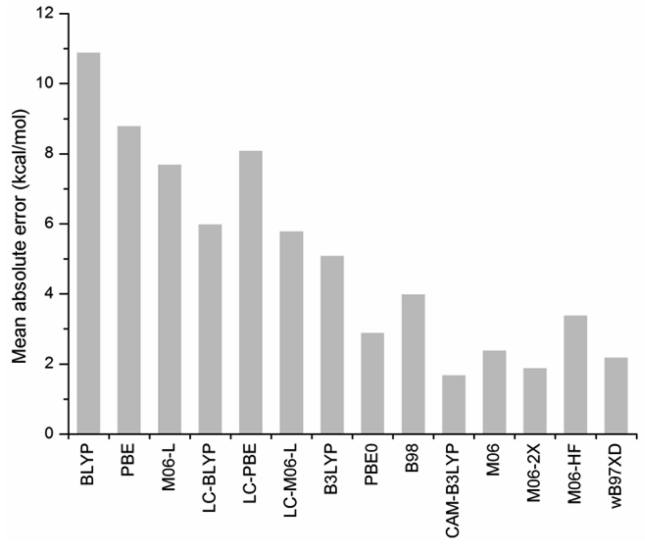

Figure 2. Mean absolute errors relative to CCSD(T) results.

Conventional hybrid functionals (B3LYP, PBE0, B98) display a better accuracy for describing phosphodiester bond cleavages as compared to pure functionals; nevertheless, they still give too low activation energies. In particular, the B3LYP method, which has been widely used in this research field, gives an underestimation of the barrier by ∼7 kcal/mol. It is remarkable that long-range corrected hybrid functionals CAM-B3LYP and ωB97XD and the one-electron self-interaction error-free hybrid meta functional M06-2X performs quite accurate in predicting the energy barriers of C3′−O and C5′−O bond cleavages that involve medium-range electron transfer; the errors of these functionals were found to be within 1.5 kcal/mol. The long-range correction has been shown to be a promising way to remedy the delocalization error.[72,77,78] The present observations that inclusion of long-range correction systematically improves the performance of pure and hybrid functionals for C−O bond cleavages can thus be seen as an indication that the error indeed stems from the spurious stabilization of the electron delocalized transition states involved in these reactions.

In contrast to the distant C3′−O and C5′−O bond cleavages for which the conventional pure and hybrid functionals work

dx.doi.org/10.1021/jp506679b | J. Phys. Chem. B 2014, 118, 11137−11144

Table 3. M06-2X/6-31++G**//M06-2X/6-31+G* Adiabatic and Vertical Electron Affinities and Vertical Electron Detachment Energies (eV)[a]

	AEA	AEA_{ZPE}	VEA	VDE
Gas Phase				
3′-dCMP	0.327	0.395	−0.302	1.384
3′-dTMP	0.487	0.572	−0.148	1.556
3′-dGMP	−0.093	0.000	−0.319	1.212
3′-dAMP	−0.089	0.001	−0.514	0.983
5′-dCMP	0.042	0.144	−0.434	0.737
5′-dTMP	0.166	0.283	−0.275	0.932
5′-dGMP	−0.290	−0.173	−0.321	0.990
5′-dAMP	−0.386	−0.267	−0.438	0.498
Aqueous Phase				
3′-dCMP	1.900 (1.905)	2.022	1.432 (1.313)	2.404 (2.825)
3′-dTMP	2.040 (2.075)	2.145	1.630 (1.528)	2.558 (3.029)
3′-dGMP	1.324 (1.344)	1.428	0.971 (0.960)	2.160 (2.645)
3′-dAMP	1.354 (1.528)	1.532	1.062 (1.078)	1.677 (2.501)
5′-dCMP	1.927 (1.816)	2.033	1.468 (1.418)	2.480 (2.443)
5′-dTMP	2.062 (1.991)	2.183	1.460 (1.564)	2.547 (2.653)
5′-dGMP	1.309 (1.358)	1.398	0.944 (0.938)	2.183 (2.652)
5′-dAMP	1.376 (1.363)	1.527	1.057 (1.094)	1.726 (2.153)

[a]Values in parentheses are SMD single-point calculations on gas-phase geometries.

atrociously, these functionals provide relatively reasonable results for the cleavage of adjacent glycosidic bonds. This is probably associated with the fact that the extent of electron delocalization in the transition state of C1′−N bond cleavage is relatively small and, therefore, is less affected by the self-interaction error. Long-range correction does not benefit the case of C1′−N bond cleavage; indeed, the long-range corrected functionals overcorrect the barrier height and lead to a larger error relative to the corresponding functionals without long-range correction. M06, B98, and B3LYP are the three best functionals for the C1′−N bond cleavage promoted by short-range electron transfer.

Considering the overall performance for the three bond-breaking reactions, the top three functionals are CAM-B3LYP, M06-2X, and ωB97XD, with mean absolute errors of 1.7, 1.9, and 2.2 kcal/mol, respectively. We recommend the M06-2X and ωB97XD for the study of DNA bond breaks induced by electron attachment. This is because these two functionals have also been shown to give a reliable description for π−π stacking,[72,79] the interaction that will be inevitably encountered when one would like to extend the investigated system to oligonucleotides. In the following study, we selected the M06-2X/6-31++G**//M06-2X/6-31+G* method to recalculate the electron attachment to nucleotides and the subsequent phosphodiester C−O bond cleavages. The reliability of previous B3LYP results on the glycosidic bond ruptures has been verified by the present benchmark study; therefore, these reactions were not reinvestigated in this work.

M06-2X Results for Electron Attachment to 3′- and 5′-dXMP (X = A, G, T, C). The computed adiabatic electron affinities (AEAs) and vertical electron affinities (VEAs) for nucleotides and the vertical detachment energies (VDEs) for the radical anions of nucleotides are listed in Table 3. The associated singly occupied molecular orbitals (SOMOs) are given in the Supporting Information (Figures S1 and S2).

The gas-phase VEAs for all nucleotides were estimated to be negative. Inspection of the SOMOs reveals that the vertically formed radical anions (i.e., electron attachment to neutral geometries) of nucleotides, except 5′-dGMP$^{\bullet-}$ and 5′-dAMP$^{\bullet-}$, are mainly characterized by valence-type anions where the excess electron occupies the π* orbital of nucleobases with more or less mixing with dipole bound or continuum states. In contrast, the SOMOs of vertical electron attachment to 5′-dGMP and 5′-dAMP display a dipole bound character.[80] Upon geometry relaxation, the excess electron becomes localized on the π* orbital of nucleobases for all nucleotides. The AEAs of dCMP (0.395 and 0.144 eV) and dTMP (0.572 and 0.283 eV) were found to be substantially positive, indicating that the corresponding valence anions are stable against electron autodetachment. On the contrary, the calculations predicted that the AEAs of 3′-dGMP and 3′-dAMP are close to zero and the 5′-dGMP and 5′-dAMP have negative AEAs of −0.173 and −0.267 eV, respectively. According to these results, it seems unlikely that the canonical forms of valence anions of purine nucleotides (dGMP$^{\bullet-}$ and dAMP$^{\bullet-}$) can stably exist in the gas phase. We would like to mention that the valence anions of 5′-dAMP have been successfully generated and studied by photoelectron spectroscopy.[81] However, the formation of these stable anions involves an intramolecular proton transfer from the phosphate group to the adenine moiety, as suggested by the computational study.[82] We also notice that the AEAs and VDEs of 3′-dXMP are larger than those of 5′-dXMP due to the presence of O5′−H···base anion interactions in the former (cf. Figure S1, Supporting Information).[44]

It is not surprising, as has been shown by many computational studies,[44,46−50,53,54] that a hydration environment greatly enhances the stability of the valence anions of nucleotides. The aqueous-phase VEAs and AEAs were estimated to fall in the ranges of 0.9−1.6 and 1.4−2.2 eV, respectively. We notice that the AEAs of pyrimidine nucleotides (2.0−2.2 eV) are larger than the negative value of ΔG_f^0 of the hydrated electron (37.5 kcal/mol or 1.6 eV),[83] indicating that the transfer of the hydrated electron to pyrimidine nucleotides is thermodynamically favorable.

M06-2X Results for C−O Bond Cleavages of 3′- and 5′-dXMP$^{\bullet-}$ (X = A, G, T, C). The computed activation energies and reaction energies of phosphodiester C−O bond cleavages induced by electron attachment to nucleotides are summarized

dx.doi.org/10.1021/jp506679b | J. Phys. Chem. B 2014, 118, 11137−11144

Table 4. M06-2X/6-31++G//M06-2X/6-31+G* Activation Energies, Activation Free Energies (kcal/mol), and Rate Constants (s^{-1}) for Phosphodiester Bond Cleavages Induced by Electron Attachment[a,b]**

	C3′−O			C5′−O		
	E^*	G^*	k	E^*	G^*	k
Gas Phase						
3′- or 5′-dCMP	23.9	20.3	4.4×10^{-2}	20.2	18.6	7.7×10^{-1}
3′- or 5′-dTMP	23.5	19.4	2.0×10^{-1}	24.4	20.9	1.6×10^{-2}
3′- or 5′-dGMP	17.8	15.0	3.3×10^{2}	16.6	13.8	2.5×10^{3}
3′- or 5′-dAMP	19.4	15.9	7.3×10^{1}	18.2	14.8	4.7×10^{2}
Aqueous Phase						
3′- or 5′-dCMP	28.5 (24.7)	28.1	8.3×10^{-8}	28.9 (17.9)	27.4	2.7×10^{-7}
3′- or 5′-dTMP	30.1 (21.7)	28.6	3.6×10^{-8}	34.2 (19.7)	32.5	5.0×10^{-11}
3′- or 5′-dGMP	14.9 (22.4)	12.5	2.3×10^{4}	16.7 (21.1)	12.5	2.3×10^{4}
3′- or 5′-dAMP	16.3 (16.8)	17.0	1.1×10^{1}	18.1 (15.4)	17.2	8.1

[a]Values in parentheses are SMD single-point calculations on gas-phase geometries. [b]Rate constants are estimated by $k = \nu_{C-O} \times e^{-G^*/RT}$, where the C−O bond vibrational frequency ν_{C-O} is assumed to be 1100 cm^{-1} and T = 298.15 K.

in Tables 4 and 5. All of these bond-breaking reactions were predicted to be substantially exergonic and hence thermodynamically favorable in both the gas phase and aqueous solution. This conclusion is consistent with the previous B3LYP calculations, although the reaction energies derived from the two methods are somewhat different. In the following discussion, we will focus on the activation energies where the M06-2X and the B3LYP give very different results.

Table 5. M06-2X/6-31++G//M06-2X/6-31+G* Reaction Energies and Reaction Free Energies (kcal/mol) for Phosphodiester Bond Cleavages Induced by Electron Attachment[a]**

	C3′−O		C5′−O	
	E_{rxn}	G_{rxn}	E_{rxn}	G_{rxn}
Gas Phase				
3′- or 5′-dCMP	−12.2	−15.6	−22.1	−23.3
3′- or 5′-dTMP	−11.6	−15.0	−19.8	−21.6
3′- or 5′-dGMP	−23.7	−27.5	−27.9	−31.4
3′- or 5′-dAMP	−23.2	−26.3	−38.4	−41.6
Aqueous				
3′- or 5′-dCMP	−21.6 (−17.1)	−24.0	−17.7 (−17.6)	−21.6
3′- or 5′-dTMP	−18.0 (−14.4)	−21.4	−14.8 (−12.5)	−16.8
3′- or 5′-dGMP	−35.9 (−30.0)	−39.8	−32.6 (−27.5)	−36.9
3′- or 5′-dAMP	−34.8 (−27.5)	−35.7	−29.7 (−30.8)	−31.9

[a]Values in parentheses are SMD single-point calculations on gas-phase geometries.

The gas-phase activation energies for the C3′−O bond cleavages were estimated to be in the range of 17.8−23.9 kcal/mol, and those for the C5′−O bond cleavages were estimated to fall in the range of 16.6−24.4 kcal/mol. The energy barriers predicted by the present M06-2X calculations are considerably higher than those reported by the previous B3LYP studies (6.2−11.2 kcal/mol for C3′−O bond and 10.0−14.3 kcal/mol for C5′−O bond; see Table 1). These results show that the underestimation of the activation energies of C−O bond cleavages triggered by electron transfer from the nucleobase to sugar−phosphate backbone is a general result for all nucleotides, not only limited to thymine nucleotides investigated in the benchmark study. It is remarkable that the M06-2X-calculated activation energies of C−O bond cleavages are comparable to the activation energies of glycosidic C−N bond cleavages predicted by the previous B3LYP calculations (18.9−24.1 kcal/mol; see Table 1), suggesting that these two bond-breaking pathways are competitive. This result is supported by the thin-film and gas-phase experiments in which both C−O and C1′−N bond cleavages were observed.[8−12] Moreover, the C−O bonds of purine nucleotides (dGMP and dAMP) were found to be somewhat more vulnerable to electron attachment compared to pyrimidine nucleotides (dCMP and dTMP); the C−O bond-breaking activation energies are 16.6−19.4 kcal/mol for purine nucleotides and 20.2−24.4 kcal/mol for pyrimidine nucleotides. This might be associated with the fact that the excess electron on purine bases is more loosely bound than that on pyrimidine bases (see electron affinities in Table 3) and, therefore, is more easily transferred to the sugar−phosphate backbone and trigger the C−O bond rupture.

We also found that the gas-phase activation energies of C3′−O bond breaking in 3′-dXMP$^{\bullet-}$ are somewhat larger than those of C5′−O bond breaking in 5′-dXMP$^{\bullet-}$. This is partly due to the formation of the O5′−H···base anion H-bonding interactions in the 3′-dXMP$^{\bullet-}$. To examine this effect, we calculated the C3′−O bond-breaking activation energies for the modified 3′-dXMP$^{\bullet-}$, where the O5′−H is replaced by a hydrogen atom (Table S2, Supporting Information). The results showed that without the O5′−H···base anion intramolecular H-bonding, the energy barriers of C3′−O bond cleavages will be lowered by ∼3−4 kcal/mol (except for 3′-dGMP$^{\bullet-}$, for which the barrier is only reduced by 0.7 kcal/mol) and become smaller than those of C5′−O bond cleavages, consistent with the trend predicted by the previous B3LYP calculations for 3′,5′-dXDP$^{\bullet-}$.

The aqueous environment was found to display quite different influences on the C−O bond-breaking activation energies for pyrimidine nucleotides and purine nucleotides; hydration tends to significantly increase the activation energies for dCMP$^{\bullet-}$ and dTMP$^{\bullet-}$ (28.5−34.2 kcal/mol in solution versus 20.2−24.4 kcal/mol in the gas phase) but has minor effects on or slightly decreases the activation energies for dGMP$^{\bullet-}$ and dAMP$^{\bullet-}$ (14.9−18.1 kcal/mol in solution versus 16.6−19.4 kcal/mol in the gas phase). A recent aqueous-phase study using femtosecond time-resolved laser spectroscopy observed the occurrence of fast dissociation (in a few picoseconds) in dGMP$^{\bullet-}$ and dTMP$^{\bullet-}$ but not in dAMP$^{\bullet-}$ and dCMP$^{\bullet-}$. In addition, the observation of similar dissociation behavior in nucleobase radical anion G$^{\bullet-}$ led the authors to deduce that the dissociation in nucleotide radical anions does not involve electron transfer from the nucleobase

dx.doi.org/10.1021/jp506679b | J. Phys. Chem. B 2014, 118, 11137−11144

to sugar−phosphate backbone (i.e., C−O bond rupture) but, instead, directly takes place at nucleobase moieties.[36] This inference is partially supported by our calculations that indicate that the C−O bond-breaking path of dTMP$^{\bullet-}$ and dCMP$^{\bullet-}$ is prohibited in the aqueous solution due to the high-energy barriers (28.5−34.2 kcal/mol). Furthermore, despite that C−O bond breaks of dGMP$^{\bullet-}$ and dAMP$^{\bullet-}$ were predicted to have moderate activation energies of 14.9−18.1 kcal/mol, the reactions with activation energies in this range are unlikely to take place on picosecond time scales (see the estimated rate constants in Table 4). For the dGMP$^{\bullet-}$, one of the possible dissociation paths responsible for the experimental observations is the glycosidic bond cleavage. This conjecture comes from the previous B3LYP calculations that predict an activation energy of 10 kcal/mol for the C1′−N bond cleavage of dGMP$^{\bullet-}$ in aqueous solution (Table 1); this energy barrier is further reduced to 7 kcal/mol upon free-energy correction.[47] It should be noted that the stability of dAMP$^{\bullet-}$ and dCMP$^{\bullet-}$ may also stem from the rapid protonation on A$^{\bullet-}$ and C$^{\bullet-}$ moieties by surrounding water, as has already been pointed out in refs 48 and 75.

We notice that the aqueous-phase activation energies derived from the geometry optimizations with the SMD solvation model and from the SMD single-point energy calculations on the gas-phase geometries (values in parentheses in Table 4) are very different for some systems. For example, the activation energies estimated by these two methods are 28.9 versus 17.9 kcal/mol for 5′-dCMP$^{\bullet-}$, 30.1 versus 21.7 kcal/mol for 3′-dTMP$^{\bullet-}$, 34.2 versus 19.7 kcal/mol for 5′-dTMP$^{\bullet-}$, and 14.9 versus 22.4 kcal/mol for 3′-dGMP$^{\bullet-}$. These results suggest the importance of using aqueous-phase geometries in the study of electron-attachment-induced DNA strand breaks.

CONCLUSIONS

In this work, we present a DFT benchmark study for the energy barriers of C−O bond cleavages in 3′- and 5′-dTMP$^{\bullet-}$ and C1′−N bond cleavage in dT$^{\bullet-}$. It was found that the conventional pure and hybrid functionals display a relatively good performance for the C1′−N bond cleavages but, on the contrary, give too low activation energies for the C−O bond-breaking reactions. The failure of conventional DFT methods in describing the C−O bond cleavages is attributed to the fact that the electron distribution of the transition states of these reactions is very delocalized and prone to be overstabilized due the self-interaction error. The long-range corrected CAM-B3LYP and ωB97XD and self-interaction error-free M06-2X are three functionals suitable for this type of bond-breaking reactions; the errors relative to the CCSD(T) results are within 1.5 kcal/mol.

The electron attachment to 3′- and 5′-dXMP (X = A, G, T, C) and the subsequent C−O bond ruptures were reinvestigated at the M06-2X/6-31++G**//M06-2X/6-31+G* level. In the gas phase, while the VEAs for all nucleotides are negative (−0.148 to −0.514 eV), the AEAs of pyrimidine nucleotides (dCMP and dTMP) are positive (0.144−0.572 eV), indicating that the gas-phase valence anions of pyrimidine nucleotides should be stable. In contrast, the purine nucleotides (dGMP and dAMP) possess almost zero and negative AEAs (0 to −0.267 eV); as a result, it seems impossible to generate the valence anions of purine nucleotides in the gas-phase experiments. In the aqueous solution, the VEAs and AEAs of nucleotides significantly increase to 0.9−1.6 and 1.4−2.2 eV, respectively.

Our calculations revealed that the C−O bonds of purine nucleotides are more susceptible than those of pyrimidine nucleotides to electron attachment. This is probably because the electron on purine bases is more loosely bound and, thus, more easily to be transferred to the sugar−phosphate backbone. The gas-phase activation energies of C−O bond cleavages are within 20.2−24.4 kcal/mol for dCMP$^{\bullet-}$ and dTMP$^{\bullet-}$ and within 16.6−19.4 kcal/mol for dGMP$^{\bullet-}$ and dAMP$^{\bullet-}$. Incorporation of the bulk hydration environment by the SMD solvation model greatly raises the C−O bond-breaking barriers of dCMP$^{\bullet-}$ and dTMP$^{\bullet-}$ to 28.5−34.2 kcal/mol, rendering these reactions virtually impossible to take place in aqueous solution. On the other hand, the corresponding energy barriers of dGMP$^{\bullet-}$ and dAMP$^{\bullet-}$ slightly decrease to 14.9−18.1 kcal/mol in the presence of water. The activation energies reported in this work are substantially higher than the previous B3LYP results, indicating that DNA strand breaks through the formation of base-centered radical anions followed by electron transfer to the sugar−phosphate backbone do not occur as easily as previously thought.

Another possible mechanism of LEE-induced DNA strand breaks is direct localization of an excess electron on the DNA backbone.[12,59,84] Using time-dependent DFT calculations, Sevilla and co-workers demonstrated that in the gas phase, the dissociative σ^* states of phosphate groups can be vertically accessible by electrons of 1−2 eV, which in turn trigger DNA strand breaks.[59,84] However, the energies of these dissociative σ^* states are significantly raised by ∼2 eV in the aqueous solution, suggesting that hydration would reduce the strand breaks of DNA by LEEs.[84] More recently, Cauët and co-workers performed DFT quantum mechanics/molecular mechanics simulations and the analyses of electronic and nuclear Fukui functions for DNA in aqueous solution.[85] They found that the forces on atomic nuclei resulting from vertical electron attachment on the DNA backbone are already large enough to trigger instantaneous DNA strand breaks within a 15−30 fs time scale; in other words, DNA strand breaks can take place before electron localization on nucleobases. Nevertheless, such an ultrafast DNA bond dissociation process has not been directly observed in quantum dynamics simulations yet, and this mechanism still waits to be verified.

ASSOCIATED CONTENT

Supporting Information

M06-2X/6-31++G** results, C3′−O bond-breaking barriers for modified 3′-dXMP$^{\bullet-}$, and singly occupied molecular orbitals. This material is available free of charge via the Internet at http://pubs.acs.org.

AUTHOR INFORMATION

Corresponding Author

*E-mail: hychen@kmu.edu.tw. Fax: +886 7 3125339. Tel: +886 7 3121101, Ext. 2807.

Notes

The authors declare no competing financial interest.

ACKNOWLEDGMENTS

We thank the Ministry of Science and Technology of Taiwan for financial support and the National Center for High-performance Computing for computer time and facilities.

REFERENCES

(1) Michael, B. D.; O'Neill, P. A Sting in the Tail of Electron Tracks. *Science* **2000**, *287*, 1603−1604.
(2) von Stonntag, C. *Free-Radical-Induced DNA Damage and Its Repair: A Chemical Perspective*; Springer: Berlin, Germany, 2006.
(3) Burrows, C. J.; Muller, J. G. Oxidative Nucleobase Modifications Leading to Strand Scission. *Chem. Rev.* **1998**, *98*, 1109−1151.
(4) Pitié, M.; Pratviel, G. Activation of DNA Carbon−Hydrogen Bonds by Metal Complexes. *Chem. Rev.* **2010**, *110*, 1018−1059.
(5) Chatgilialoglu, C.; Ferreri, C.; Terzidis, M. A. Purine 5′,8-Cyclonucleoside Lesions: Chemistry and Biology. *Chem. Soc. Rev.* **2011**, *40*, 1368−1382.
(6) Boudaïffa, B.; Cloutier, P.; Hunting, D.; Huels, M. A.; Sanche, L. Resonant Formation of DNA Strand Breaks by Low-Energy (3 to 20 eV) Electrons. *Science* **2000**, *287*, 1658−1660.
(7) Martin, F.; Burrow, P. D.; Cai, Z.; Cloutier, P.; Hunting, D.; Sanche, L. DNA Strand Breaks Induced by 0−4 eV Electrons: The Role of Shape Resonances. *Phys. Rev. Lett.* **2004**, *93*, 068101.
(8) Zheng, Y.; Cloutier, P.; Hunting, D. J.; Sanche, L.; Wagner, J. R. Chemical Basis of DNA Sugar−Phosphate Cleavage by Low-Energy Electrons. *J. Am. Chem. Soc.* **2005**, *127*, 16592−16598.
(9) Zheng, Y.; Wagner, J. R.; Sanche, L. DNA Damage Induced by Low-Energy Electrons: Electron Transfer and Diffraction. *Phys. Rev. Lett.* **2006**, *96*, 208101.
(10) Zheng, Y.; Cloutier, P.; Sanche, L.; Wagner, J. R. Low Energy Electron Induced DNA Damage: Effects of Terminal Phosphate and Base Moieties on the Distribution of Damage. *J. Am. Chem. Soc.* **2008**, *130*, 5612−5613.
(11) Li, Z.; Cloutier, P.; Sanche, L.; Wagner, J. R. Low-Energy Electron-Induced DNA Damage: Effect of Base Sequence in Oligonucleotide Trimers. *J. Am. Chem. Soc.* **2010**, *132*, 5422−5427.
(12) Kopyra, J. Low Energy Electron Attachment to the Nucleotide Deoxycytidine Monophosphate: Direct Evidence for the Molecular Mechanisms of Electron-Induced DNA Strand Breaks. *Phys. Chem. Chem. Phys.* **2012**, *14*, 8287−8289.
(13) Bald, I.; Dabkowska, I.; Illenberger, E. Probing Biomolecules by Laser-Induced Acoustic Desorption: Electrons at Near Zero Electron Volts Trigger Sugar−Phosphate Cleavage. *Angew. Chem., Int. Ed.* **2008**, *47*, 8518−8520.
(14) Zheng, Y.; Cloutier, P.; Hunting, D. J.; Wagner, J. R.; Sanche, L. Glycosidic Bond Cleavage of Thymidine by Low-Energy Electrons. *J. Am. Chem. Soc.* **2004**, *126*, 1002−1003.
(15) Abdoul-Carime, H.; Gohlke, S.; Fischbach, E.; Scheike, J.; Illenberger, E. Thymine Excision from DNA by Subexcitation Electrons. *Chem. Phys. Lett.* **2004**, *387*, 267−270.
(16) Ptasińska, S.; Denifl, S.; Gohlke, S.; Scheier, P.; Illenberger, E.; Märk, T. D. Decomposition of Thymidine by Low-Energy Electrons: Implications for the Molecular Mechanisms of Single-Strand Breaks in DNA. *Angew. Chem., Int. Ed.* **2006**, *45*, 1893−1896.
(17) Hanel, G.; Gstir, B.; Denifl, S.; Scheier, P.; Probst, M.; Farizon, B.; Farizon, M.; Illenberger, E.; Märk, T. D. Electron Attachment to Uracil: Effective Destruction at Subexcitation Energies. *Phys. Rev. Lett.* **2003**, *90*, 188104.
(18) Abdoul-Carime, H.; Gohlke, S.; Illenberger, E. Site-Specific Dissociation of DNA Bases by Slow Electrons at Early Stages of Irradiation. *Phys. Rev. Lett.* **2004**, *92*, 168103.
(19) Ptasińska, S.; Denifl, S.; Scheier, P.; Illenberger, E.; Märk, T. D. Bond- and Site-Selective Loss of H Atoms from Nucleobases by Very-Low-Energy Electrons. *Angew. Chem., Int. Ed.* **2005**, *44*, 6941−6943.
(20) Abdoul-Carime, H.; Langer, J.; Huels, M. A.; Illenberger, E. Decomposition of Purine Nucleobases by Very Low Energy Electrons. *Eur. Phys. J. D* **2005**, *35*, 399−404.
(21) Scheer, A. M.; Aflatooni, K.; Gallup, G. A.; Burrow, P. D. Bond Breaking and Temporary Anion States in Uracil and Halouracils: Implications for the DNA Bases. *Phys. Rev. Lett.* **2004**, *92*, 068102.
(22) Ptasińska, S.; Denifl, S.; Grill, V.; Märk, T. D.; Illenberger, E.; Scheier, P. Bond- and Site-Selective Loss of H^- from Pyrimidine Bases. *Phys. Rev. Lett.* **2005**, *95*, 093201.
(23) Ptasińska, S.; Denifl, S.; Grill, V.; Märk, T. D.; Scheier, P.; Gohlke, S.; Huels, M. A.; Illenberger, E. Bond-Selective H^- Ion Abstraction from Thymine. *Angew. Chem., Int. Ed.* **2005**, *44*, 1647−1650.
(24) Li, X.; Cai, Z.; Sevilla, M. D. Investigation of Proton Transfer within DNA Base Pair Anion and Cation Radicals by Density Functional Theory (DFT). *J. Phys. Chem. B* **2001**, *105*, 10115−10123.
(25) Gu, J.; Xie, Y.; Schaefer, H. F. Electron Attachment Induced Proton Transfer in a DNA Nucleoside Pair: 2′-Deoxyguanosine-2′-deoxycytidine. *J. Chem. Phys.* **2007**, *127*, 155107.
(26) Chen, H. Y.; Kao, C. L.; Hsu, S. C. N. Proton Transfer in Guanine−Cytosine Radical Anion Embedded in B-Form DNA. *J. Am. Chem. Soc.* **2009**, *131*, 15930−15938.
(27) Chen, H. Y.; Hsu, S. C. N.; Kao, C. L. Microhydration of 9-Methylguanine:1-Methylcytosine Base Pair and Its Radical Anion: A Density Functional Theory Study. *Phys. Chem. Chem. Phys.* **2010**, *12*, 1253−1263.
(28) Chen, H. Y.; Yeh, S. W.; Kao, C. L.; Hsu, S. C. N.; Dong, T. Y. Effect of Nucleobase Sequence on the Proton-Transfer Reaction and Stability of the Guanine−Cytosine Base Pair Radical Anion. *Phys. Chem. Chem. Phys.* **2011**, *13*, 2674−2681.
(29) Hsu, S. C. N.; Wang, T. P.; Kao, C. L.; Chen, H. F.; Yang, P. Y.; Chen, H. Y. Theoretical Study of the Protonation of the One-Electron-Reduced Guanine−Cytosine Base Pair by Water. *J. Phys. Chem. B* **2013**, *117*, 2096−2105.
(30) Szyperska, A.; Rak, J.; Leszczynski, J.; Li, X.; Ko, Y. J.; Wang, H.; Bowen, K. H. Valence Anions of 9-Methylguanine−1-Methylcytosine Complexes. Computational and Photoelectron Spectroscopy Studies. *J. Am. Chem. Soc.* **2009**, *131*, 2663−2669.
(31) Kumar, A.; Sevilla, M. D. Proton-Coupled Electron Transfer in DNA on Formation of Radiation-Produced Ion Radicals. *Chem. Rev.* **2010**, *110*, 7002−7023.
(32) Ptasińska, S.; Denifl, S.; Scheier, P.; Märk, T. D. Inelastic Electron Interaction (Attachment/Ionization) with Deoxyribose. *J. Chem. Phys.* **2004**, *120*, 8505.
(33) Sulzer, P.; Ptasińska, S.; Zappa, F.; Mielewska, B.; Milosavljevic, A. R.; Scheier, P.; Märk, T. D.; Bald, I.; Gohlke, S.; Huels, M. A.; Illenberger, E. Dissociative Electron Attachment to Furan, Tetrahydrofuran, and Fructose. *J. Chem. Phys.* **2006**, *125*, 044304.
(34) Bald, I.; Kopyra, J.; Illenberger, E. Selective Excision of C5 from D-Ribose in the Gas Phase by Low-Energy Electrons (0−1 eV): Implications for the Mechanism of DNA Damage. *Angew. Chem., Int. Ed.* **2006**, *45*, 4851−4855.
(35) von Stonntag, C. *The Chemical Basis of Radiation Biology*; Taylor and Francis: London, 1987.
(36) Wang, C. R.; Nguyen, J.; Lu, Q. B. Bond Breaks of Nucleotides by Dissociative Electron Transfer of Nonequilibrium Prehydrated Electrons: A New Molecular Mechanism for Reductive DNA Damage. *J. Am. Chem. Soc.* **2009**, *131*, 11320−11322.
(37) Nguyen, J.; Ma, Y.; Luo, T.; Bristow, R. G.; Jaffray, D. A.; Lu, Q. B. Direct Observation of Ultrafast-Electron-Transfer Reactions Unravels High Effectiveness of Reductive DNA Damage. *Proc. Natl. Acad. Sci. U.S.A.* **2011**, *108*, 11778−11783.
(38) Sanche, L. Beyond Radical Thinking. *Nature* **2009**, *461*, 358−359.
(39) Barrios, R.; Skurski, P.; Simons, J. Mechanism for Damage to DNA by Low-Energy Electrons. *J. Phys. Chem. B* **2002**, *106*, 7991−7994.
(40) Berdys, J.; Skurski, P.; Simons, J. Damage to Model DNA Fragments by 0.25−1.0 eV Electrons Attached to a Thymine π^* Orbital. *J. Phys. Chem. B* **2004**, *108*, 5800−5805.
(41) Berdys, J.; Anusiewicz, I.; Skurski, P.; Simons, J. Theoretical Study of Damage to DNA by 0.2−1.5 eV Electrons Attached to Cytosine. *J. Phys. Chem. A* **2004**, *108*, 2999−3005.
(42) Berdys, J.; Anusiewicz, I.; Skurski, P.; Simons, J. Damage to Model DNA Fragments from Very Low-Energy (<1 eV) Electrons. *J. Am. Chem. Soc.* **2004**, *126*, 6441−6447.
(43) Simons, J. How Do Low-Energy (0.1−2 eV) Electrons Cause DNA-Strand Breaks? *Acc. Chem. Res.* **2006**, *39*, 772−779.

(44) Bao, X.; Wang, J.; Gu, J.; Leszczynski, J. DNA Strand Breaks Induced by Near-Zero-Electronvolt Electron Attachment to Pyrimidine Nucleotide. *Proc. Natl. Acad. Sci. U.S.A.* **2006**, *103*, 5658−5663.
(45) Gu, J.; Wang, J.; Leszczynski, J. Electron Attachment-Induced DNA Single Strand Breaks: $C_{3'}$−$O_{3'}$ σ-Bond Breaking of Pyrimidine Nucleotides Predominates. *J. Am. Chem. Soc.* **2006**, *128*, 9322−9323.
(46) Gu, J.; Wang, J.; Leszczynski, J. Electron Attachment-Induced DNA Single-Strand Breaks at the Pyrimidine Sites. *Nucleic Acids Res.* **2010**, *38*, 5280−5290.
(47) Gu, J.; Wang, J.; Leszczynski, J. Comprehensive Analysis of DNA Strand Breaks at the Guanosine Site Induced by Low-Energy Electron Attachment. *ChemPhysChem* **2010**, *11*, 175−181.
(48) Gu, J.; Wang, J.; Leszczynski, J. Low Energy Electron Attachment to the Adenosine Site of DNA. *J. Phys. Chem. B* **2011**, *115*, 14831−14837.
(49) Kumar, A.; Sevilla, M. D. Low-Energy Electron Attachment to 5′-Thymidine Monophosphate: Modeling Single Strand Breaks Through Dissociative Electron Attachment. *J. Phys. Chem. B* **2007**, *111*, 5464−5474.
(50) Xie, H.; Wu, R.; Xia, F.; Cao, Z. Effects of Electron Attachment on $C_{5'}$−$C_{5'}$ and $C_{1'}$−N_1 Bond Cleavages of Pyrimidine Nucleotides: A Theoretical Study. *J. Comput. Chem.* **2008**, *29*, 2025−2032.
(51) Schyman, P.; Laaksonen, A. On the Effect of Low-Energy Electron Induced DNA Strand Break in Aqueous Solution: A Theoretical Study Indicating Guanine as a Weak Link in DNA. *J. Am. Chem. Soc.* **2008**, *130*, 12254−12255.
(52) Gu, J.; Xie, Y.; Schaefer, H. F. Glycosidic Bond Cleavage of Pyrimidine Nucleosides by Low-Energy Electrons: A Theoretical Rationale. *J. Am. Chem. Soc.* **2005**, *127*, 1053−1057.
(53) Gu, J.; Leszczynski, J.; Schaefer, H. F. Interactions of Electrons with Bare and Hydrated Biomolecules: From Nucleic Acid Bases to DNA Segments. *Chem. Rev.* **2012**, *112*, 5603−5640.
(54) Zhang, R. b.; Zhang, K.; Eriksson, L. A. Theoretical Studies of Damage to 3′-Uridine Monophosphate Induced by Electron Attachment. *Chem.—Eur. J.* **2008**, *14*, 2850−2856.
(55) Li, X.; Sanche, L.; Sevilla, M. D. Base Release in Nucleosides Induced by Low-Energy Electrons: A DFT Study. *Radiat. Res.* **2006**, *165*, 721−729.
(56) Li, X.; Sevilla, M. D.; Sanche, L. Density Functional Theory Studies of Electron Interaction with DNA: Can Zero eV Electrons Induce Strand Breaks? *J. Am. Chem. Soc.* **2003**, *125*, 13668−13669.
(57) Cohen, A. J.; Mori-Sánchez, P.; Yang, W. Insights into Current Limitations of Density Functional Theory. *Science* **2008**, *321*, 792−794.
(58) Cohen, A. J.; Mori-Sánchez, P.; Yang, W. Challenges for Density Functional Theory. *Chem. Rev.* **2012**, *112*, 289−320.
(59) Kumar, A.; Sevilla, M. D. The Role of $\pi\sigma^*$ Excited States in Electron-Induced DNA Strand Break Formation: A Time-Dependent Density Functional Theory Study. *J. Am. Chem. Soc.* **2008**, *130*, 2130−2131.
(60) Becke, A. D. Density-Functional Exchange-Energy Approximation with Correct Asymptotic Behavior. *Phys. Rev. A* **1988**, *38*, 3098−3100.
(61) Lee, C.; Yang, W.; Parr, R. G. Development of the Colle−Salvetti Correlation-Energy Formula into a Functional of the Electron Density. *Phys. Rev. B* **1988**, *37*, 785−789.
(62) Perdew, J. P.; Burke, K.; Ernzerhof, M. Generalized Gradient Approximation Made Simple. *Phys. Rev. Lett.* **1996**, *77*, 3865−3868.
(63) Perdew, J. P.; Burke, K.; Ernzerhof, M. Errata: Generalized Gradient Approximation Made Simple. *Phys. Rev. Lett.* **1997**, *78*, 1396.
(64) Zhao, Y.; Truhlar, D. G. A New Local Density Functional for Main-Group Thermochemistry, Transition Metal Bonding, Thermochemical Kinetics, and Noncovalent Interactions. *J. Chem. Phys.* **2006**, *126*, 194101.
(65) Becke, A. D. Density-Functional Thermochemistry. III. The Role of Exact Exchange. *J. Chem. Phys.* **1993**, *98*, 5648−5652.
(66) Adamo, C.; Barone, V. Toward Reliable Density Functional Methods without Adjustable Parameters. *J. Chem. Phys.* **1999**, *110*, 6158−6170.
(67) Schmider, H. L.; Becke, A. D. Optimized Density Functionals from the Extended G2 Test Set. *J. Chem. Phys.* **1998**, *108*, 9624−9631.
(68) Zhao, Y.; Truhlar, D. G. The M06 Suite of Density Functionals for Main Group Thermochemistry, Thermochemical Kinetics, Noncovalent Interactions, Excited States, and Transition Elements. *Theor. Chem. Acc.* **2008**, *120*, 215−241.
(69) Zhao, Y.; Truhlar, D. G. Density Functional for Spectroscopy: No Long-Range Self-Interaction Error, Good Performance for Rydberg and Charge-Transfer States, and Better Performance on Average than B3LYP for Ground States. *J. Phys. Chem. A* **2006**, *110*, 13126−13130.
(70) Iikura, H.; Tsuneda, T.; Yanai, T.; Hirao, K. Long-Range Correction Scheme for Generalized-Gradient-Approximation Exchange Functionals. *J. Chem. Phys.* **2001**, *115*, 3540−3544.
(71) Yanai, T.; Tew, D.; Handy, N. A New Hybrid Exchange−Correlation Functional Using the Coulomb-Attenuating Method (CAM-B3LYP). *Chem. Phys. Lett.* **2004**, *393*, 51−57.
(72) Chai, J. D.; Head-Gordon, M. Long-Range Corrected Hybrid Density Functionals with Damped Atom-Atom Dispersion Corrections. *Phys. Chem. Chem. Phys.* **2008**, *10*, 6615−6620.
(73) Marenich, A. V.; Cramer, C. J.; Truhlar, D. G. Universal Solvation Model Based on Solute Electron Density and on a Continuum Model of the Solvent Defined by the Bulk Dielectric Constant and Atomic Surface Tensions. *J. Phys. Chem. B* **2009**, *113*, 6378−6396.
(74) Frisch, M. J.; Trucks, G. W.; Schlegel, H. B.; Scuseria, G. E.; Robb, M. A.; Cheeseman, J. R.; Scalmani, G.; Barone, V.; Mennucci, B.; Petersson, G. A.; et al. *Gaussian 09*, revision A.02; Gaussian, Inc.: Wallingford, CT, 2009.
(75) Smyth, M.; Kohanoff, J. Excess Electron Interactions with Solvated DNA Nucleotides: Strand Breaks Possible at Room Temperature. *J. Am. Chem. Soc.* **2012**, *134*, 9122−9125.
(76) Schyman, P.; Laaksonen, A.; Hugosson, H. W. Phosphodiester Bond Rupture in 5′ and 3′ Cytosine Monophosphate in Aqueous Environment and the Effect of Low-Energy Electron Attachment: A Car−Parrinello QM/MM Molecular Dynamics Study. *Chem. Phys. Lett.* **2008**, *462*, 289−294.
(77) Baer, R.; Livshits, E.; Salzner, U. Tuned Range-Separated Hybrids in Density Functional Theory. *Annu. Rev. Phys. Chem.* **2010**, *61*, 85−109.
(78) Heaton-Burgess, T.; Yang, W. Structural Manifestation of the Delocalization Error of Density Functional Approximation: C_{4N+2} Rings and C_{20} Bowl, Cage, and Ring Isomers. *J. Chem. Phys.* **2010**, *132*, 234113.
(79) Zhao, Y.; Truhlar, D. G. Density Functionals with Broad Applicability in Chemistry. *Acc. Chem. Res.* **2008**, *41*, 157−167.
(80) Li, X.; Cai, Z.; Sevilla, M. D. DFT Calculations of the Electron Affinities of Nucleic Acid Bases: Dealing with Negative Electron Affinities. *J. Phys. Chem. A* **2002**, *106*, 1596−1603.
(81) Stokes, S. T.; Grubisic, A.; Li, X.; Ko, Y. J.; Bowen, K. H. Photoelectron Spectroscopy of the Parent Anions of the Nucleotides, Adenosine-5′-Monophosphate and 2′Deoxyadenosine-5′-Monophosphate. *J. Chem. Phys.* **2008**, *128*, 044314.
(82) Kobyłecka, M.; Gu, J.; Rak, J.; Leszczynski, J. Barrier-Free Proton Transfer in the Valence Anion of 2′-Deoxyadenosine-5′-Monophosphate. II. A Computational Study. *J. Chem. Phys.* **2008**, *128*, 044315.
(83) Jortner, J.; Nyoes, R. M. Some Thermodynamic Properties of the Hydrated Electron. *J. Phys. Chem.* **1966**, *70*, 770−774.
(84) Kumar, A.; Sevilla, M. D. Role of Excited States in Low-Energy Electron (LEE) Induced Strand Breaks in DNA Model Systems: Influence of Aqueous Environment. *ChemPhysChem* **2009**, *10*, 1426−1430.
(85) Cauët, E.; Bogatko, S.; Liévin, J.; De Profit, F.; Geerlings, P. Electron-Attachment-Induced DNA Dagame: Instantaneous Strand Breaks. *J. Phys. Chem. B* **2013**, *117*, 9669−9676.